RAD18 Is a Maternal Limiting Factor Silencing the UV-Dependent DNA Damage Checkpoint in Xenopus Embryos

Chames Kermi, Susana Prieto, Siem Van der laan, Nikolay Tsanov, Bénédicte Recolin, Emmanuelle Uro-Coste, Marie-Bernadette Delisle, Domenico Maiorano

Graphical Abstract

Click here to download Graphical Abstract: Graphical abstract.tif

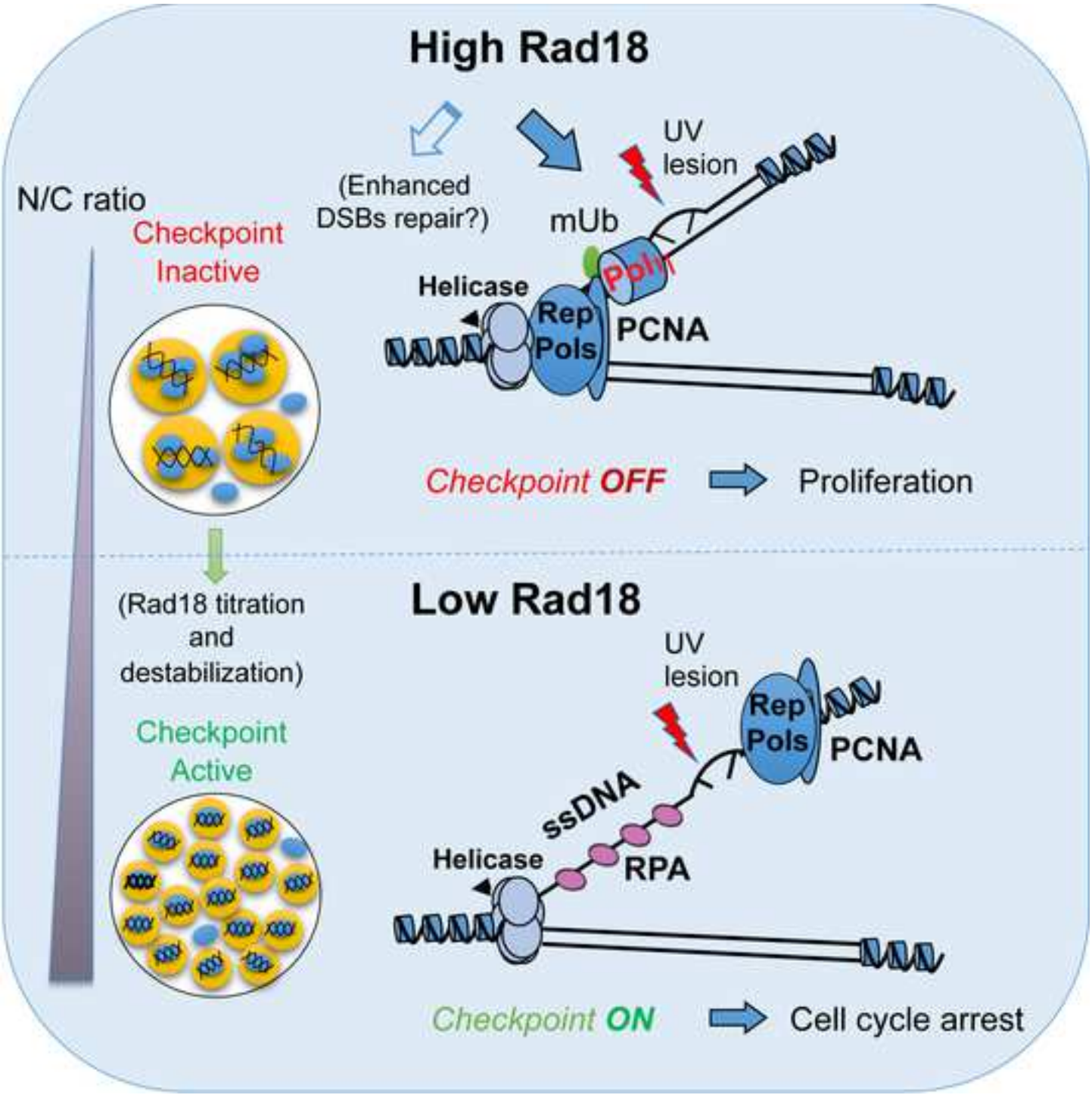

Rad18 is a maternal limiting factor silencing the UV-dependent DNA damage checkpoint in *Xenopus* embryos

Chames Kermi[1,7], Susana Prieto[1,2,7], Siem van der Laan[1,3], Nikolay Tsanov[1,4], Bénédicte Recolin[1,5], Emmanuelle Uro-Coste[6], Bernadette Delisle[6] and Domenico Maiorano[1,8]

Affiliations:

[1]Genome Surveillance and Stability Laboratory, CNRS-UPR1142. Institute of Human Genetics, 141, rue de la Cardonille. 34396 Cedex 5, Montpellier-France.

[2]Present address: Institute of Molecular Genetics of Montpellier. 1919 Route de Mende. 34296 Montpellier Cedex 5.

[3]Present address: CNRS UMR3145. Parc Euromedicine Cap Delta. 1682 rue de la Valsiere 34184 Montpellier, France.

[4]Present address: Centre for Chromosome Biology. National University of Ireland Galway

[5]Present address : Medical Research Council Laboratory of Molecular Biology, Francis Crick Avenue, Cambridge. CB2 OQH, UK.

[6]Laboratoire Universitaire d'Anatomie Pathologique. Faculté de Médecine Rangueil. Université Toulouse III. CHU, INSERM . 1, avenue Jean Poulhès. CS 53717 Toulouse, France.

[7]Co-first author.

[8]Corresponding author. Contact information: CNRS-UPR1142. Institute of Human Genetics. 141, rue de la Cardonille. 34396 Cedex 5 Montpellier, France.

Tel. : +33 (0) 4 34 35 99 73

Fax : +33 (0) 4 34 35 99 01

Email : domenico.maiorano@igh.cnrs.fr

Running title: DNA damage checkpoint control by Rad18

Summary

In early embryos the DNA damage checkpoint is silent until the midblastula transition (MBT) due to maternal-limiting factors of unknown identity. Here, we identify the Rad18 ubiquitin ligase as one such factor in *Xenopus*. We show, *in vitro* and *in vivo*, that inactivation of Rad18 function leads to DNA damage-dependent checkpoint activation, monitored by Chk1 phosphorylation. Moreover, we show that the abundance of both Rad18 and PCNA monoubiquitylated (mUb) are developmentally-regulated. Increased DNA abundance limits availability of Rad18 close to MBT thereby reducing $PCNA^{mUb}$ and inducing checkpoint derepression. Further, we show that this embryonic-like regulation can be reactivated in somatic mammalian cells by ectopic Rad18 expression thus conferring resistance to DNA damage. Finally, we find high Rad18 expression in cancer stem cells highly resistant to DNA damage. Altogether these data propose Rad18 as a critical embryonic checkpoint-inhibiting factor and suggest that Rad18 deregulation may have an unexpected oncogenic potential.

Introduction

Early embryonic cleavages are rapid, consisting of alternating S- and M-phases, with virtually absent Gap-phases (Graham and Morgan, 1966). In this contracted cell cycle, the S-phase checkpoint delaying cell division upon DNA damage (Anderson et al., 1997; Hensey and Gautier, 1997) or unreplicated DNA (Dasso and Newport, 1990; Kimelman et al., 1987) is inefficient and may represent an adaptation to ensure rapid proliferation. The molecular mechanisms responsible for checkpoint inhibition in early embryos are poorly understood. Previous studies in *Xenopus* (Conn et al., 2004; Dasso and Newport, 1990; Kappas et al., 2000) have shown that checkpoint activation depends upon the nuclear-to-cytoplasmic (N/C) ratio, due to absence of cell growth, and not upon transcription nor translation, suggesting titration of maternal limiting factors of unknown identity. Genetic data in *C. elegans* (Holway et al., 2006; Ohkumo et al., 2006) have implicated a translesion DNA polymerase (TLS Polη) specialized in replication of damaged DNA (Sale et al., 2012, for review). Polη is recruited to DNA damage upon binding to PCNA, monoubiquitylated by the Rad6 (E2)-Rad18(E3) ubiquitin ligase complex while the USP1 ubiquitin hydrolase catalyzes the opposite reaction (Ulrich and Takahashi, 2013, for review). In S-phase, checkpoint activation relies upon replication fork uncoupling generated by DNA damage such as UV-irradiation. Excess single-stranded (ss)DNA, generated in this process by the action of the helicase, is the primary substrate initiating ATR-dependent checkpoint signaling (Byun et al., 2005). Here we provide evidence that checkpoint repression in *Xenopus* eggs is a consequence of replication fork uncoupling inhibition mediated by Rad18, a critical factor for $PCNA^{mUb}$. We also show that this regulation is reversible and can be reactivated by increasing

Rad18 abundance, resulting in resistance to DNA damaging agents that is relevant to cancer recurrence.

Results and Discussion

Constitutive TLS Polη binding to chromatin at low N/C ratio

To understand the molecular grounds of embryonic checkpoint silencing, we used *cell-free* extracts derived from activated *Xenopus* eggs. This *in vitro* system faithfully reproduces the developmentally-regulated activation of the DNA damage checkpoint observed *in vivo* (Anderson et al., 1997; Conn et al., 2004; Kappas et al., 2000; Newport and Dasso, 1989). This is achieved by adding a sufficient amount of sperm nuclei into a fixed volume of egg cytoplasm thus reaching a critical N/C ratio that triggers checkpoint activation (400 nuclei/μl, Dasso and Newport, 1990).

Figure S1A-C shows that UV-irradiated sperm nuclei, added at low N/C ratio into egg extracts naturally synchronized in very early S-phase, fail to delay both DNA synthesis and mitotic entry, compared to high N/C ratio. Consistent with previous observations *in vivo* (Conn et al., 2004; Kappas et al., 2000), we did not observe Chk1 phosphorylation at low N/C ratio (Figure 1A, upper panel, lane 2) while this occurred normally at high N/C ratio, as expected (Kumagai et al., 1998). Inhibition of Chk1 phosphorylation was also observed using a fixed amount of damaged sperm nuclei while increasing the extract volume (Figure S1D), thus strengthening the conclusion that checkpoint activation is sensitive to the N/C ratio and not to the total amount of DNA damage.

Using as readout for replication fork uncoupling the ssDNA binding protein RPA

(Recolin et al., 2012; Walter and Newport, 2000) we observed that RPA greatly accumulated onto chromatin in S-phase at high N/C ratio upon UV-irradiation, as expected, (Figure 1A; lower panel, lane 4), while RPA accumulation was strongly reduced at low N/C ratio (lane 2), suggesting inefficient replication fork uncoupling. This is consistent with previous observations in *C. elegans* embryos (Holway et al., 2006; Ohkumo et al., 2006) as well as with reduced production of ssDNA in human embryonic stem cells (Desmarais et al., 2012). In addition, UV-dependent accumulation of the ATR-Interacting Protein (ATRIP), recruited by RPA and required for checkpoint signaling, was also strongly abolished, while it was recruited normally at high N/C ratio. At low N/C ratio, ATR was bound to chromatin and showed modest accumulation upon UV-irradiation, similar to ATRIP. Efficient replication fork uncoupling is observed at low N/C ratio by blocking DNA synthesis with aphidicolin, an inhibitor of replicative DNA polymerases (Figure S1E), suggesting that the uncoupling defect is specific to UV-damage. Interestingly, at low N/C ratio we observed that Polη is chromatin-associated with or without DNA damage (Figure 1A, lower panel, lanes 1-2). In contrast, at high N/C ratio Polη was recruited only after UV-irradiation (lanes 3-4). We have also verified the presence of replicative polymerases on chromatin at low N/C ratio (Figure S1F) and observed that Polη abundance is similar to that of Polα (Figure S1G). Strikingly, at low N/C ratio, $PCNA^{mUb}$ was observed on chromatin irrespective of DNA damage (Figure 1A, lanes 1-2), while at high N/C ratio $PCNA^{mUb}$ was present mainly upon UV irradiation (lane 4, lower panel), as previously reported (Chang et al., 2006). Damage-independent Polη recruitment at low N/C ratio was reduced by addition of Geminin, an inhibitor of replication fork formation (Figure S1H), suggesting replication fork dependency for

binding. Since TLS Polη replicates past UV lesions, constitutive Polη binding may avoid forks stalling by UV lesions, thus preventing replication fork uncoupling and ssDNA formation. In turn, this leads to failure to recruit checkpoint factors (ATRIP) and precludes checkpoint activation. Constitutive TLS in early embryos may be important to tolerate not only external damage but also endogenous replication stress induced by high concentration of nucleotides. This possibility is in line with evidence suggesting that rNTPs incorporation causes replication stress and induces $PCNA^{mUb}$ in yeast, and that TLS activity is required for replication resumption (Lazzaro et al., 2012).

Rad6-Rad18 and not Polη is titrated from egg cytosol at high N/C ratio

Maternally-supplied inhibitor(s), present in limited amount in egg cytoplasm and progressively titrated on chromatin during embryonic cleavages may be responsible for checkpoint silencing (Conn et al., 2004; Dasso and Newport, 1990; Kappas et al., 2000, and Graphical Abstract). Data shown in Figure 1A, and previous data in *C. elegans* (Holway et al., 2006; Ohkumo et al., 2006), implicate TLS components. We analyzed the abundance of several TLS factors remaining in the cytoplasm after incubation with sperm nuclei at low or high N/C ratio and observed that USP1, Polη, PCNA, RPA, Chk1, and ATR levels did not change (Figure 1B and Figure S1I), suggesting that they are in excess over the DNA. By raising specific antibodies (Figure S2A), we observed that Rad6 and Rad18 were depleted from the extract and less abundant on chromatin at high N/C ratio (Figure 1B). Reduced Rad18 and Rad6 chromatin binding at high N/C ratio correlates with both reduced $PCNA^{mUb}$ and Polη chromatin binding in the absence of UV-damage, while USP1 binding did not significantly change, suggesting that Rad18

may be limiting near MBT. To investigate whether this is due to titration or destabilization, we analyzed Rad18 binding to chromatin at increasing N/C ratios, with or without the proteasome inhibitor MG132 (Figure S2B, upper panel) and observed a gradual decline in both conditions suggesting titration, although MG132 increased Rad18 abundance at high N/C ratio. Moreover, kinetic analysis of chromatin binding *in vitro* shows that Rad18 is absent from chromatin at the end of S-phase (Figure S2B, lower panel), while in presence of MG132 its abundance is increased, suggesting destabilization after replication. Altogether these results suggest that both titration and destabilization limit the availability of Rad18 at high N/C ratio.

In mammalian cells, Rad18 is recruited to chromatin upon DNA damage by physical interactions with the Dbf4 subunit of the Cdc7 protein kinase (Yamada et al., 2013). Interestingly, immunoprecipitation experiments show complex formation between Rad18 and the *Xenopus* Dbf4-related protein Drf1 at low N/C ratio, in the absence of damage (Figure 1C). This complex was virtually undetectable at high N/C ratio, even when an excess of Rad18 immunoprecipitates, compared to low N/C ratio, were analyzed (Figure 1C, right panel). This observation suggests that at low N/C ratio high Rad18 abundance promotes DNA damage-independent complex formation with Drf1, to constitutively target Rad18 to replication forks.

Rad18 and PCNA^{mUb} are developmentally-regulated

Analysis of Rad18 and PCNA^{mUb} abundance in embryos at different stages of development shows that Rad18 decreases during embryogenesis, starting from stage 4, and drops to very low levels at stage 6.5 (pre-MBT, Figure 1D). Rad18 decline is

paralleled by a correspondent decrease in PCNA^{mUb}. Similar to what observed *in vitro* (Figure S2B), injection of MG132 into embryos, at a dose that does not interfere with the timing of MBT onset (Brandt et al., 2011), did not affect the decline of Rad18 levels prior to stage 6, although it significantly increased Rad18 abundance at stage 6.5 (Figure 1E). This result suggests that *in vivo* both titration and destabilization limit Rad18 abundance near MBT. In contrast, Drf1 did not show significant changes up to stage 7, similar to what previously reported (Collart et al., 2013; Takahashi and Walter, 2005), suggesting that Rad18 is more limiting than Drf1. This possibility is supported by the observation that Drf1 is not depleted from egg cytoplasm at high N/C ratio (Figure S1I) and is consistent with Drf1 titration at a higher N/C ratio (around 3000 nuclei/μl, Collart et al., 2013), while onset of the DNA damage checkpoint occurs at 400 nuclei/μl (Conn et al., 2004; Dasso and Newport, 1990; Kappas et al., 2000). Hence, reduced Rad18 abundance and not Drf1 is likely responsible for DNA damage-dependent checkpoint activation, although it cannot be excluded that titration of Rad18 stabilizing factor(s) may also contribute. Quantification of Rad18 shows that its concentration in *Xenopus* eggs is relatively low (~ 0.25 ng/embryo, 3.5 nM; Figure S2C), over one thousand times less than PCNA. Genetic evidence in *C. elegans* proposed Polη as a repressor of the checkpoint (Holway et al., 2006; Ohkumo et al., 2006; Roerink et al., 2012). Although we find that in *Xenopus* Polη is implicated, it is not limiting since it is not quantitatively depleted at high N/C ratio. We speculate that at high N/C ratio, reduced abundance of Rad18 may be counteracted by USP1 resulting in reduced PCNA^{mUb}.

Rad6-Rad18 inhibits the UV-dependent DNA damage checkpoint *in vitro* at low N/C ratio

We next removed Rad18 from egg extracts using specific antibodies. As expected (Bailly et al., 1994), Rad18 depletion also partially removed Rad6 (Figure 2A, lane 2; Figure S2D), but not Polη, RPA, or PCNA. Rad18 depletion drastically reduced $PCNA^{mUb}$ upon UV-irradiation at low N/C ratio, as well as Polη chromatin binding, and importantly, induced UV-damage-dependent Chk1 phosphorylation (Figure 2B, lane 3). In contrast, Rad18 depletion at high N/C ratio did not induce checkpoint hyper activation compared to a mock-depletion (Figure S2E), indicating that this phenotype is specific to low N/C ratio, and likely it is not due to accumulation of unrepaired DNA as neither Rad6 nor Rad18 are required for Nucleotide Excision Repair (Hishida et al., 2009). Moreover, pre- and post-MBT embryos appear to have similar DNA repair capacity (Anderson et al., 1997). Further, the N/C ratio, and not the total amount of damaged DNA, is critical for checkpoint activation (Conn et al., 2004), ruling out differences in DNA repair rates.

Reconstitution of Rad18-depleted extracts at low N/C ratio (Figure S2F) with a recombinant 6His-Rad6-Rad18 complex (Figure 2C) inhibited UV-damage-dependent Chk1 phosphorylation (Figure 2D, lane 5), excluding the implication of co-depleted proteins. Further, this complex, and not recombinant Rad6 rescued defective $PCNA^{mUb}$ in Rad18-depleted extracts, demonstrating that it is functional (Figure S2G). Furthermore, Chk1 phosphorylation was induced by UV-damage when recombinant $PCNA^{K164R}$ mutant that cannot be monoubiquitylated, and not wild-type PCNA (WT), was added to extracts at low N/C ratio (Figure S2H). Of note, the recently discovered

Primpol (Helleday, 2013, for review), was not bound to chromatin at low N/C ratio (Figure S2I), ruling out active UV lesions bypass, or replication fork restart by this polymerase. Finally, recombinant 6His-Rad6-Rad18 repressed both RPA accumulation and Chk1 phosphorylation normally observed at high N/C ratio upon UV-irradiation (Figure 2E, compare lanes 2 and 3), suggesting inhibition of replication fork uncoupling.

Rad18 silences the UV-dependent DNA damage checkpoint in *Xenopus* embryos

To obtain evidence for checkpoint inhibition by Rad18 *in vivo*, we overexpressed either $Rad18^{WT}$ or catalytic inactive Rad18 (C28F mutant) by microinjection of the corresponding mRNA into embryos at the 2-cell stage. Embryos injected with either water (Mock) or $Rad18^{WT}$ mRNA developed normally and reached stage 6.5 with or without UV-irradiation (Figure 2F). In contrast, UV-irradiated embryos injected with $Rad18^{C28F}$ were delayed in the embryonic cleavages from one cell cycle after UV-irradiation (Figure S2J). Consistent with this phenotype, UV-irradiated embryos expressing the $Rad18^{C28F}$ mutant accumulated Chk1 phosphorylation while expression of $Rad18^{WT}$ inhibited it (Figure 2G, compare lane 3 with lane 4). Importantly, no spontaneous Chk1 phosphorylation was observed in embryos injected with either Rad18 mRNAs (Figure S2K, -UV) showing that Rad18 is not implicated in DNA damage-independent developmental activation of Chk1, as reported for Drf1 (Collart et al., 2013). These data altogether show that Rad18 inhibition is sufficient to give to the embryo the competence to activate the DNA damage checkpoint. Since Rad18 is also implicated in double strand break repair (Huang et al., 2009; Szuts et al., 2006; Watanabe et al., 2009), it might also contribute to silencing the checkpoint upon

γ-irradiation, although we have not tested this possibility.

Reactivation of embryonic-like checkpoint silencing in mammalian cells by Rad18 upregulation

Next we analyzed the consequences of increasing Rad18 abundance in somatic mammalian cells. Rad18 overexpression did not induce significant cell cycle changes (Figure S3A), and consistent with two previous reports (Bi et al., 2006; Davies et al., 2008) induced constitutive $PCNA^{mUb}$ (Figure 3A). Importantly, overexpression of either Rad6, or Rad18 and Rad6, was not sufficient to induce constitutive $PCNA^{mUb}$ to a level similar to that of Rad18 alone (Figure S3B). Of note, and unlike what observed in *Xenopus* at low N/C ratio (Figure 1A), the amount of $PCNA^{mUb}$ observed in asynchronous cells expressing Rad18, increased after UV irradiation. Moreover, eGFP-Polη nuclear foci formed even in the absence of DNA damage only upon Rad18 overexpression (Figure 3B-C). Most importantly, UV-dependent Chk1 phosphorylation was significantly reduced in asynchronous cells expressing Rad18 (Figure 3D; Figure S3D) suggesting that in mammalian cells high Rad18 abundance is sufficient to inhibit UV-dependent checkpoint activation, in line with a previous observation in yeast (Daigaku et al., 2010). A very similar result was obtained upon expression of $PCNA^{K164R}$ fused to ubiquitin (Figure 3E-F) that mimics constitutive $PCNA^{mUb}$ (Kanao et al., 2015). Moreover, expression of Rad18 lacking Cdc7 phosphorylation sites ($Rad18^{\Delta 401-445}$), also required for Polη binding (Durando et al., 2013), did not induce constitutive eGFP-Polη nuclear foci and acts as a dominant negative since it inhibits eGFP-Polη foci formation after UV-damage (Figure S3C), consistent with a previous report (Day et al., 2010). This

mutant did not inhibit Chk1 phosphorylation compared to Rad18^{WT} (Figure S3D), suggesting that checkpoint silencing depends upon Rad18 phosphorylation by Cdc7. Similarly, the TLS-deficient Rad18^{C28F} mutant did not induce constitutive eGFP-Polη nuclear foci (Figure S3E). Finally, and entirely consistent with results in *Xenopus* (Figure 1A), high Rad18 expression also strongly repressed RPA foci formed upon UV irradiation in mammalian cells (Figure 4A), suggesting inhibition of replication fork uncoupling. Altogether these observations show that Rad18 overexpression is sufficient to induce constitutive PCNA^{mUb} independently of Rad6, although we could not formally prove it in *Xenopus*, since we failed to express active recombinant Rad18 without Rad6. This suggests that when overexpressed Rad18 may either bypass the Rad6 requirement, or Rad18 may use another abundant E2 to catalyze PCNA^{mUb}. This latter possibility may explain why in *C. elegans* Rad6 mutations did not delay mitotic entry in early embryos upon DNA damage (Holway et al., 2006).

We next determined whether cells expressing Rad18 display increased resistance to DNA damage resulting from impaired checkpoint activation. To this end, we generated stable cell lines expressing ectopic Rad18 at a similar level to endogenous Rad18. Expression of Rad18^{WT} significantly increased cell viability upon exposure to either UV-irradiation or to the chemotherapy-relevant drug cisplatin, while Rad18^{C28F} did not (Figure 4B-C). Taken together these results link Rad18 expression to checkpoint inactivation and resistance to DNA damaging agents.

Rad18 is overexpressed in cancer stem cells highly resistant to DNA damage

Resistance to DNA damaging agents is linked to cancer recurrence. We observed high Rad18 expression in a colon cancer-derived cell line resistant to oxaliplatin (HCT116) compared to the HCT8 sensitive cancer cell line (Figure S4A), as well as in the highly DNA damage-resistant brain cancer glioblastoma (Figure 4D). Importantly, we observed high Rad18 expression specifically in glioblastoma cancer stem cells isolated from tumor biopsies ($CD133^{+}$), and not in their differentiated counterparts that express Rad18 to similar levels than HeLa cells (Figure 4E). In contrast expression of Rad6 and of other TLS-, checkpoint- and proliferation-relevant proteins was not increased in glioblastoma (Figure S4B). This result is consistent with GEO Profiles data showing high Rad18 mRNA expression in glioblastoma cancer stem cells. Moreover, very recent data implicate Rad18 in therapeutic resistance of colon cancer cells (Liu et al., 2015). Further, Rad18 downregulation in the U87 glioblastoma cell line induced sensitivity to cisplatin (Figure 4F) while Rad18 re-expression induced a dramatic increased viability, suggesting acquired resistance. Since glioblastoma is resistant to cisplatin, this observation puts forward Rad18 as a target for sensitizing glioblastoma to cisplatin. Altogether our findings suggest that increased Rad18 expression has a positive effect on proliferation upon DNA damage by shunting checkpoint activation thus conferring resistance to DNA damage (see Graphical abstract), and show high Rad18 expression specifically in cancer stem cells that are implicated in the resistance to therapy.

In conclusion, this work suggests that constitutive $PCNA^{mUb}$, driven by Rad18, is responsible for silencing the UV-damage checkpoint in *Xenopus* embryos by inhibiting replication fork uncoupling, a critical determinant for checkpoint signaling. Genetic data in *C. elegans* (Holway et al., 2006; Ohkumo et al., 2006), and the presence of

constitutive PCNA^{mUb} in early *Drosophila* embryos (our unpublished observation), makes likely that this regulation may be conserved in other organisms. Recent data suggest that the DNA damage checkpoint affects TLS through regulation of a Rad18-Cdc7-Dbf4 complex (Yamada et al., 2013). Our observations show that Rad18 deregulation affects the DNA damage checkpoint, suggesting a cross talk between these two pathways. This may constitute an additional mechanism, aside from the mutator activity, linking TLS deregulation to cancer (Albertella et al., 2005). In this perspective, Rad18 deregulation might have a previously unrecognized oncogenic potential relevant to the therapeutic resistance of certain cancer subtypes, such as those of embryonic origin or those generated by dedifferentiation of somatic cells.

Experimental Procedures

Xenopus egg extracts preparation and use

Experiments with *Xenopus* were performed in accordance with current institutional and national regulations approved by the Minister of Research under supervision of the Departmental Direction of Population Protection (DDPP). Interphasic and cycling *Xenopus* egg extracts were prepared and used as described (Murray, 1991; Recolin et al., 2012). UV-irradiation of sperm chromatin and isolation of chromatin fractions was as described (Recolin et al., 2012).

Xenopus embryos and microinjection experiments

Embryos were prepared by *in vitro* fertilization using standard procedures (Sivel, 2000), UV-irradiated at the 2-cell stage and microinjected with the indicated mRNAs. Total protein extracts were obtained by collecting staged embryos according to Nieuwkoop and Faber normal tables.

mRNA synthesis

In vitro transcription was performed using mMESSAGE mMACHINE Kit® (Ambion). mRNA was ethanol-precipitated and dissolved in water ready for microinjection.

Cell culture

Cells were cultured and maintained under standard conditions. For transient expression, HEK293T were transfected with calcium phosphate. Twenty-four hours post transfection cells were mock- or UV-irradiated and collected at indicated time points. Whole cell extracts were clarified by centrifugation.

Immunofluorescence microscopy and foci formation assay

Cells were grown on coverslips prior to co-transfection. Four hours after UV-C irradiation, cells were fixed with 3.2 % paraformaldehyde for 15 min at room temperature and washed three times with PBS. After washing twice with PBS + 3% BSA, cells were mounted with ProlongGold DAPI (Invitrogen). eGFP-Polη foci were analyzed with Leica DM6000 epifluorescence microscope (RIO imaging facility). Images were acquired using a Coolsnap HQ CCD camera (Photometrics) and metamorph

software (Molecular Devices). The percentage of eGFP-Polη- expressing cells displaying eGFP-Polη foci was determined by scoring at least 200 nuclei for each condition. Nuclei containing under 30 foci were scored as negatives.

Generation of stable NIH3T3 cells expressing Rad18

Cells were infected with viral particles generated by transfecting Platinum-E ecotropic packaging cell line (Cell Biolabs) with retroviral vectors (pLPC-puro) encoding Rad18 variants (WT, C28F) using Lipofectamine® (Invitrogen). The viral supernatant was collected to infect cells. Forty-eight hours post infection, cells were selected in puromycin (2.5 μg/ml, Sigma)-containing medium. Selected populations were expanded and promptly used.

Cell viability experiments

Cells were plated at 1.0 x 10^4 per well in twelve-well plates and UV-irradiated or exposed to the indicated amount of cisplatin. 48 hours post irradiation, cell viability was determined using the CellTiter-Glo® Luminescent Cell Viability assay (Promega).

siRNA

U87 cells were co-transfected either with siRNA using JETPrime reagent (Polyplus). Twenty-four hours after transfection, cells were trypsinized and seeded in 12 wells plates at 10^4 cells/well density. Twenty-four hours later cells were treated with cisplatin (Sigma).

Statistical methods

Unless otherwise stated, data are presented as mean values ± SD of three independent experiments. For data shown in Figures 1E, 3F, 4B, S2B, S3E, and S4B, unpaired, two-tailed *t* test were performed. *p* values are represented (***p<0.0001, **p<0.001, *p<0.01). All statistical analyses were calculated using Graphpad® Prism 6 software. Significance was assumed when $p < 0.01$.

Authors contribution

Conceptualization D.M.; Methodology; D.M. and C.K.; Validation C.K.; Formal Analysis, C.K. and S.v.d.L.; Original Draft, D.M.; Review & Editing, D.M., C.K., B.R., & S.P.; Investigation, D.M., C.K., S.P. B.R., N.T., S.v.d.L.; Supervision D.M., Funding Acquisition, D.M.; Resources, E.U-C. & B.D.

Acknowledgements

We thank M. Méchali for encouragement, J. Moreau for help with microinjection and M. Lamers for Rad-Rad18 purification, P. Coulombe for help with stable cell lines, A. Eloualid for technical assistance, K. Cimprich for XRad18 cDNA, P. Kannouche for eGFP-Polη, C. Vaziri for Rad18$^{\Delta 401\text{-}445}$, C. Masutani for PCNA-Ubiquitin, M. Akiyama (XPolη), A. Kumagai & W. Dunphy (XDrf1), J. Huang (Primpol) for antibodies, P-H. Nasheuer for the gift of recombinant Polα, J. Sale & J. Hutchins for critical reading of

the manuscript. Grants supporting this work were from ARC (N° 3156), FRM (DEQ20071210543), Ligue contre le Cancer (to C.K.) and ANR (CHECKDEV). None of the authors of this manuscript have a financial interest related to this work.

References

Albertella, M.R., Lau, A., and O'Connor, M.J. (2005). The overexpression of specialized DNA polymerases in cancer. DNA Repair (Amst) *4*, 583-593.

Anderson, J.A., Lewellyn, A.L., and Maller, J.L. (1997). Ionizing radiation induces apoptosis and elevates cyclin A1-Cdk2 activity before but not after the midblastula transition in Xenopus. Mol Biol Cell *8*, 1195-1206.

Bailly, V., Lamb, J., Sung, P., Prakash, S., and Prakash, L. (1994). Specific complex formation between yeast RAD6 and RAD18 proteins: a potential mechanism for targeting RAD6 ubiquitin-conjugating activity to DNA damage sites. Genes Dev *8*, 811-820.

Bi, X., Barkley, L.R., Slater, D.M., Tateishi, S., Yamaizumi, M., Ohmori, H., and Vaziri, C. (2006). Rad18 regulates DNA polymerase kappa and is required for recovery from S-phase checkpoint-mediated arrest. Mol Cell Biol *26*, 3527-3540.

Brandt, Y., Mitchell, T., Wu, Y., and Hartley, R.S. (2011). Developmental downregulation of Xenopus cyclin E is phosphorylation and nuclear import dependent and is mediated by ubiquitination. Developmental Biology *355*, 65-76.

Byun, T.S., Pacek, M., Yee, M.C., Walter, J.C., and Cimprich, K.A. (2005). Functional uncoupling of MCM helicase and DNA polymerase activities activates the ATR-dependent checkpoint. Genes Dev *19*, 1040-1052.

Chang, D.J., Lupardus, P.J., and Cimprich, K.A. (2006). Monoubiquitination of proliferating cell nuclear antigen induced by stalled replication requires uncoupling of DNA polymerase and mini-chromosome maintenance helicase activities. J Biol Chem *281*, 32081-32088.

Collart, C., Allen, G.E., Bradshaw, C.R., Smith, J.C., and Zegerman, P. (2013). Titration of four replication factors is essential for the Xenopus laevis midblastula transition. Science *341*, 893-896.

Conn, C.W., Lewellyn, A.L., and Maller, J.L. (2004). The DNA damage checkpoint in embryonic cell cycles is dependent on the DNA-to-cytoplasmic ratio. Dev Cell *7*, 275-281.

Daigaku, Y., Davies, A.A., and Ulrich, H.D. (2010). Ubiquitin-dependent DNA damage bypass is separable from genome replication. Nature *465*, 951-955.

Dasso, M., and Newport, J.W. (1990). Completion of DNA replication is monitored by a feedback system that controls the initiation of mitosis in vitro: studies in Xenopus. Cell *61*, 811-823.

Davies, A.A., Huttner, D., Daigaku, Y., Chen, S., and Ulrich, H.D. (2008). Activation of ubiquitin-dependent DNA damage bypass is mediated by replication protein a. Mol Cell *29*, 625-636.

Day, T.A., Palle, K., Barkley, L.R., Kakusho, N., Zou, Y., Tateishi, S., Verreault, A., Masai, H., and Vaziri, C. (2010). Phosphorylated Rad18 directs DNA polymerase eta to sites of stalled replication. The Journal of cell biology *191*, 953-966.

Desmarais, J.A., Hoffmann, M.J., Bingham, G., Gagou, M.E., Meuth, M., and Andrews, P.W. (2012). Human Embryonic Stem Cells Fail to Activate CHK1 and Commit to Apoptosis in Response to DNA Replication Stress. Stem Cells *30*, 1385-1393.

Durando, M., Tateishi, S., and Vaziri, C. (2013). A non-catalytic role of DNA polymerase eta in recruiting Rad18 and promoting PCNA monoubiquitination at stalled replication forks. Nucleic acids research *41*, 3079-3093.

Graham, C.F., and Morgan, R.W. (1966). Changes in the cell cycle during early amphibian development. Developmental Biology *14*, 439-460.

Helleday, T. (2013). PrimPol breaks replication barriers. Nature structural & molecular biology *20*, 1348-1350.

Hensey, C., and Gautier, J. (1997). A developmental timer that regulates apoptosis at the onset of gastrulation. Mech Dev *69*, 183-195.
Hishida, T., Kubota, Y., Carr, A.M., and Iwasaki, H. (2009). RAD6-RAD18-RAD5-pathway-dependent tolerance to chronic low-dose ultraviolet light. Nature *457*, 612-615.
Holway, A.H., Kim, S.H., La Volpe, A., and Michael, W.M. (2006). Checkpoint silencing during the DNA damage response in Caenorhabditis elegans embryos. J Cell Biol *172*, 999-1008.
Huang, J., Huen, M.S., Kim, H., Leung, C.C., Glover, J.N., Yu, X., and Chen, J. (2009). RAD18 transmits DNA damage signalling to elicit homologous recombination repair. Nat Cell Biol *11*, 592-603.
Kanao, R., Masuda, Y., Deguchi, S., Yumoto-Sugimoto, M., Hanaoka, F., and Masutani, C. (2015). Relevance of simultaneous mono-ubiquitinations of multiple units of PCNA homo-trimers in DNA damage tolerance. PLoS One *10*, e0118775.
Kappas, N.C., Savage, P., Chen, K.C., Walls, A.T., and Sible, J.C. (2000). Dissection of the XChk1 signaling pathway in Xenopus laevis embryos. Mol Biol Cell *11*, 3101-3108.
Kimelman, D., Kirschner, M., and Scherson, T. (1987). The events of the midblastula transition in Xenopus are regulated by changes in the cell cycle. Cell *48*, 399-407.
Kumagai, A., Guo, Z., Emami, K.H., Wang, S.X., and Dunphy, W.G. (1998). The Xenopus Chk1 protein kinase mediates a caffeine-sensitive pathway of checkpoint control in cell-free extracts. J Cell Biol *142*, 1559-1569.
Lazzaro, F., Novarina, D., Amara, F., Watt, D.L., Stone, J.E., Costanzo, V., Burgers, P.M., Kunkel, T.A., Plevani, P., and Muzi-Falconi, M. (2012). RNase H and postreplication repair protect cells from ribonucleotides incorporated in DNA. Molecular cell *45*, 99-110.
Liu, R.L., Dong, Y., Deng, Y.Z., Wang, W.J., and Li, W.D. (2015). Tumor suppressor miR-145 reverses drug resistance by directly targeting DNA damage-related gene RAD18 in colorectal cancer. Tumour Biol.
Murray, A.W. (1991). Cell cycle extracts. Methods in Cell Biology *36*, 581-605.
Newport, J., and Dasso, M. (1989). On the coupling between DNA replication and mitosis. J Cell Sci Suppl *12*, 149-160.
Ohkumo, T., Masutani, C., Eki, T., and Hanaoka, F. (2006). Deficiency of the Caenorhabditis elegans DNA polymerase eta homologue increases sensitivity to UV radiation during germ-line development. Cell Struct Funct *31*, 29-37.
Recolin, B., Van der Laan, S., and Maiorano, D. (2012). Role of replication protein A as sensor in activation of the S-phase checkpoint in Xenopus egg extracts. Nucleic Acids Res *40*, 3431-3442.
Roerink, S.F., Koole, W., Stapel, L.C., Romeijn, R.J., and Tijsterman, M. (2012). A broad requirement for TLS polymerases eta and kappa, and interacting sumoylation and nuclear pore proteins, in lesion bypass during C. elegans embryogenesis. PLoS genetics *8*, e1002800.
Sale, J.E., Lehmann, A.R., and Woodgate, R. (2012). Y-family DNA polymerases and their role in tolerance of cellular DNA damage. Nat Rev Mol Cell Biol *13*, 141-152.
Sivel, H.L., Grainer, R.M., Harland, R.M. (2000). Early Development of Xenopus laevis. A laboratory manual. (New York, Cold Spring harbour Laboratory Press).
Szuts, D., Simpson, L.J., Kabani, S., Yamazoe, M., and Sale, J.E. (2006). Role for RAD18 in homologous recombination in DT40 cells. Mol Cell Biol *26*, 8032-8041.
Takahashi, T.S., and Walter, J.C. (2005). Cdc7-Drf1 is a developmentally regulated protein kinase required for the initiation of vertebrate DNA replication. Genes & development *19*, 2295-2300.
Ulrich, H.D., and Takahashi, T. (2013). Readers of PCNA modifications. Chromosoma *122*, 259-274.
Walter, J., and Newport, J. (2000). Initiation of eukaryotic DNA replication: origin unwinding and sequential chromatin association of Cdc45, RPA, and DNA polymerase alpha. Mol Cell *5*, 617-627.
Watanabe, K., Iwabuchi, K., Sun, J., Tsuji, Y., Tani, T., Tokunaga, K., Date, T., Hashimoto, M., Yamaizumi, M., and Tateishi, S. (2009). RAD18 promotes DNA double-strand break repair during G1 phase through chromatin retention of 53BP1. Nucleic Acids Res *37*, 2176-2193.
Yamada, M., Watanabe, K., Mistrik, M., Vesela, E., Protivankova, I., Mailand, N., Lee, M., Masai, H., Lukas, J., and Bartek, J. (2013). ATR-Chk1-APC/CCdh1-dependent stabilization of Cdc7-ASK (Dbf4) kinase is required for DNA lesion bypass under replication stress. Genes & development *27*, 2459-2472.

Figures legend

Figure 1. Rad18 is limiting near the MBT

(A) Constitutive Polη chromatin binding and PCNA^{mUb} at low N/C ratio. Western blot of nucleosolic (upper panel) or chromatin (lower panel) fractions obtained from egg extracts containing sperm nuclei at low (100 nuclei/μl) or high (1000 nuclei/μl) N/C ratio, UV-irradiated (+UV) or not (-UV), upon fifty minutes incubation at room temperature. Histone H3 serves as chromatin loading control.

(B) Abundance of the indicated proteins (determined by western blot) remaining in egg cytoplasm (left panel) or chromatin (right panel) after ninety minutes incubation with sperm chromatin at low or high N/C ratio.

(C) Rad18 interacts with Drf1 at low N/C ratio in *Xenopus* egg extracts. Western blot of Rad18 immunoprecipitated from egg cytoplasm after nuclear assembly at low or high N/C ratio. Short (light) and long (dark) exposures of Drf1 are shown. Ten-fold more Rad18 immunoprecipitates at low N/C ratio are also shown (right panel).

(D) Rad18 and PCNA^{mUb} are developmentally-regulated. Western blot of total embryos protein extracts at the indicated stages of development (numbers), in the absence (DMSO) or presence of the proteasome inhibitor MG132 (30 μM; **E**). Rad18

quantification is expressed as Relative Optical Density (ROD). Means and standard deviations are represented (**p <0.001; See also Figure S1).

Figure 2. Rad18 depletion induces Chk1 phosphorylation at low N/C ratio upon UV damage

(A-B) Western blot of cytoplasm (A) or chromatin fractions (B) obtained at low N/C ratio upon immunodepletion with Rad18 antibodies.

(C) Coomassie blue stain of recombinant 6His-rad6-Rad18 complex expressed and purified from insect cells. kDa indicates molecular weight of standard protein markers.

(D) Chk1 phosphorylation analyzed by western blot in either mock-depleted, or Rad18-depleted egg extracts with UV-irradiated (+ UV) or not (- UV) sperm nuclei at low N/C ratio, as well as with recombinant (^{Rec}) 6His-Rad6-Rad18. Chk1 serves here as loading control.

(E, left panel) Western blot of chromatin fractions analyzed in the absence (-) or presence (+) of UV-irradiation with or without recombinant 6His-Rad6-Rad18 complex at high N/C ratio. Reactions were incubated at room temperature for sixty minutes. **(Right panel)** Quantification of RPA2 accumulation in left panel. Numbers indicated lanes of left panel. Means and standard deviations are shown (n=3).

(F, left panel) Overexpression of Rad18^{C28F} delays embryonic cleavages. Images of stage 6.5 embryos, injected with either water (Mock), XRad18^{WT} or XRad18^{C28F} mRNA, UV-irradiated (+UV) or not (-UV). **(Right panel)** Quantification of embryos shown in left panel reaching stage 6.5 (pre-MBT). Means and standard deviations are represented (n=3).

(G) Rad18 overexpression inhibits UV-dependent Chk1 phosphorylation in *Xenopus* embryos. Western blot of protein extracts from stage 7 embryos obtained upon injection of Rad18 mRNAs (from panel F; See also Figure S2).

Figure 3. Ectopic Rad18 expression induces spontaneous TLS Polη foci and inhibits UV-dependent Chk1 phosphorylation in mammalian cells

(A) Western blot of HEK293T cell extracts obtained upon transfection with Rad18 or empty vector (pCDNA3).

(B) Expression of Rad18, and not Rad6, induces constitutive Polη foci. HEK293T cells co-transfected with the indicated vectors and eGFP-Polη were stained with DAPI to visualize DNA and observed for eGFP fluorescence. Scale bar: 10μm.

(C) Quantification of eGFP-Polη foci from the experiment described in panel B. Means and standard deviation are shown (n=3).

(D) Western blot of $Chk1^{S345}$ phosphorylation in HEK293T cells expressing empty vector or XRad18, upon UV irradiation (+UV) at the indicated times. Quantification of $Chk1^{S345}$ phosphorylation is also shown (n=2).

(E-F) Checkpoint inhibition and constitutive eGFP-Polη foci upon expression of $PCNA^{K164R}$-mUb fusion. (E) Western blot of total extracts made from HEK293T cells UV-irradiated (+UV) or not (-UV) expressing the indicated vectors. (F) Cells co-transfected with the indicated vectors and eGFP-Polη, were analyzed as described in panel (B). Scale bar: 10μm. Quantification of eGFP-Polη foci is also shown (right panel). Means and standard deviation are shown (***p<0.0001; n=3; see also Figure S3).

Figure 4. High Rad18 expression is associated with resistance to DNA damage

(A) Rad18 expression inhibits UV-dependent RPA focus formation in mammalian cells. HEK293T cells transfected with the indicated expression vectors stained with DAPI to visualize DNA, and RPA2 antibodies, were viewed by fluorescence microscopy. Scale bar: 10μm. Quantification of RPA2 foci from the experiment described in panel (A) is also shown. Means and standard deviation are shown (**$p < 0,01$; n=3).

(B) Survival curves of asynchronous NIH3T3 cells stably expressing either empty vector, low levels of $Rad18^{WT}$ or $Rad18^{C28F}$ mutant, challenged by the indicated does of UV-C or cisplatin (CisPt, panel **C**) normalized to non-irradiated cells (mock). Means and standard deviations are shown (**$p < 0,01$; n=3).

(D) Expression of Rad18 mRNA in gliospheres ($CD133^{+}$, Glioma) compared to Hela cells by RT-PCR. Means and standard deviation are shown (n=3).

(E) Western blot of total cell extracts from glioblastoma biopsies (grade 4), differentiated counterparts (progenitors, $CD133^{-}$) or Hela cells.

(F, upper panel) Western blot of U87 glioblastoma cell extracts treated with control siRNA (siLuc), a Rad18-specific siRNA (siRad18), or co-transfected with Rad18 siRNA and a plasmid expressing $Rad18^{WT}$ (siRad8 + Rad18). **(Lower panel)** Survival curves of U87 glioblastoma cells treated as described in the upper panel, challenged with the indicated doses of cisplatin (CisPt), compared to non-treated cells (mock). Means and standard deviations are shown (n=3; see also Figure S4).

Figure1

Click here to download Figure: Figure1.tif

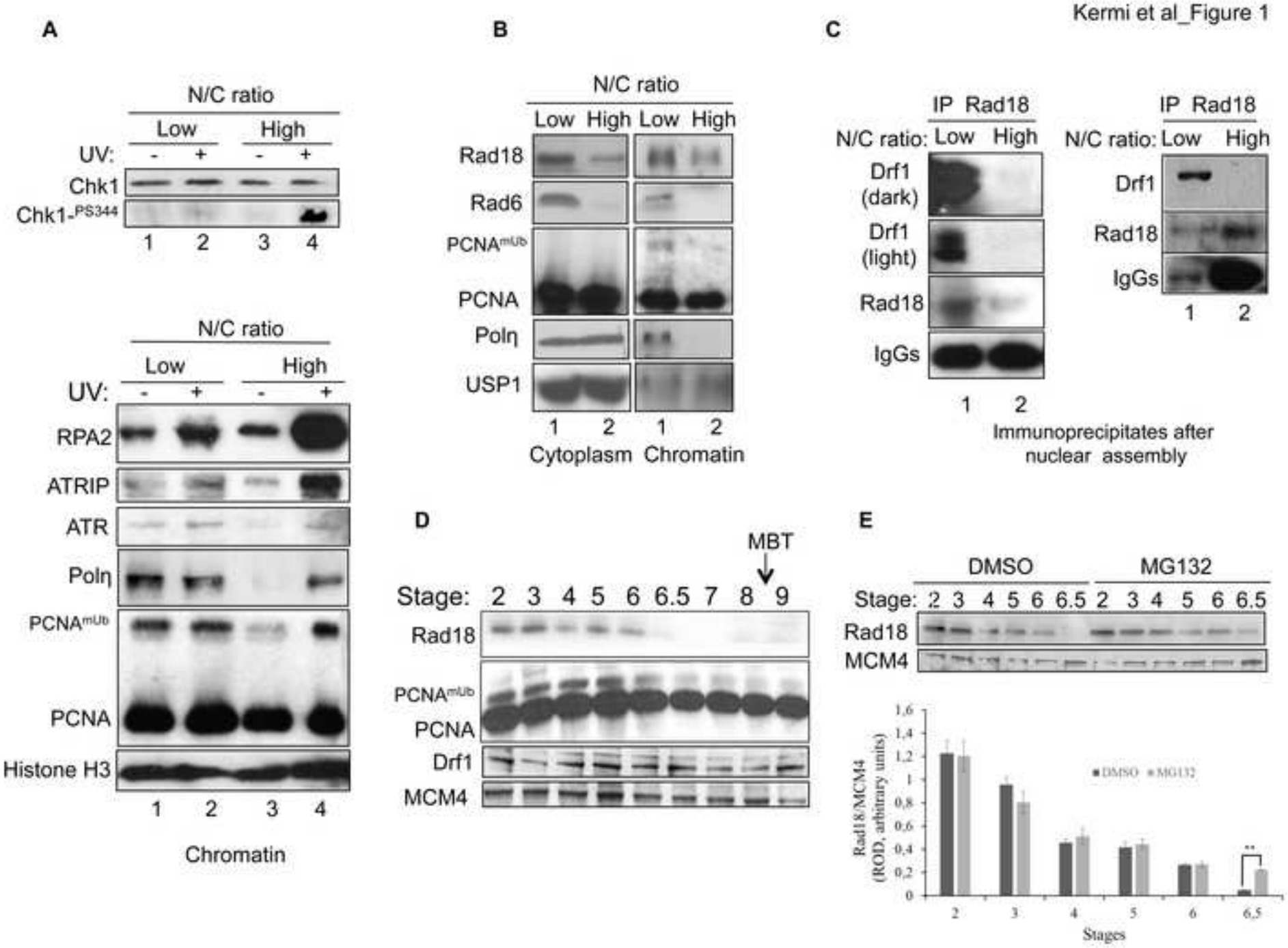

Figure2

Click here to download Figure: Figure2.tif

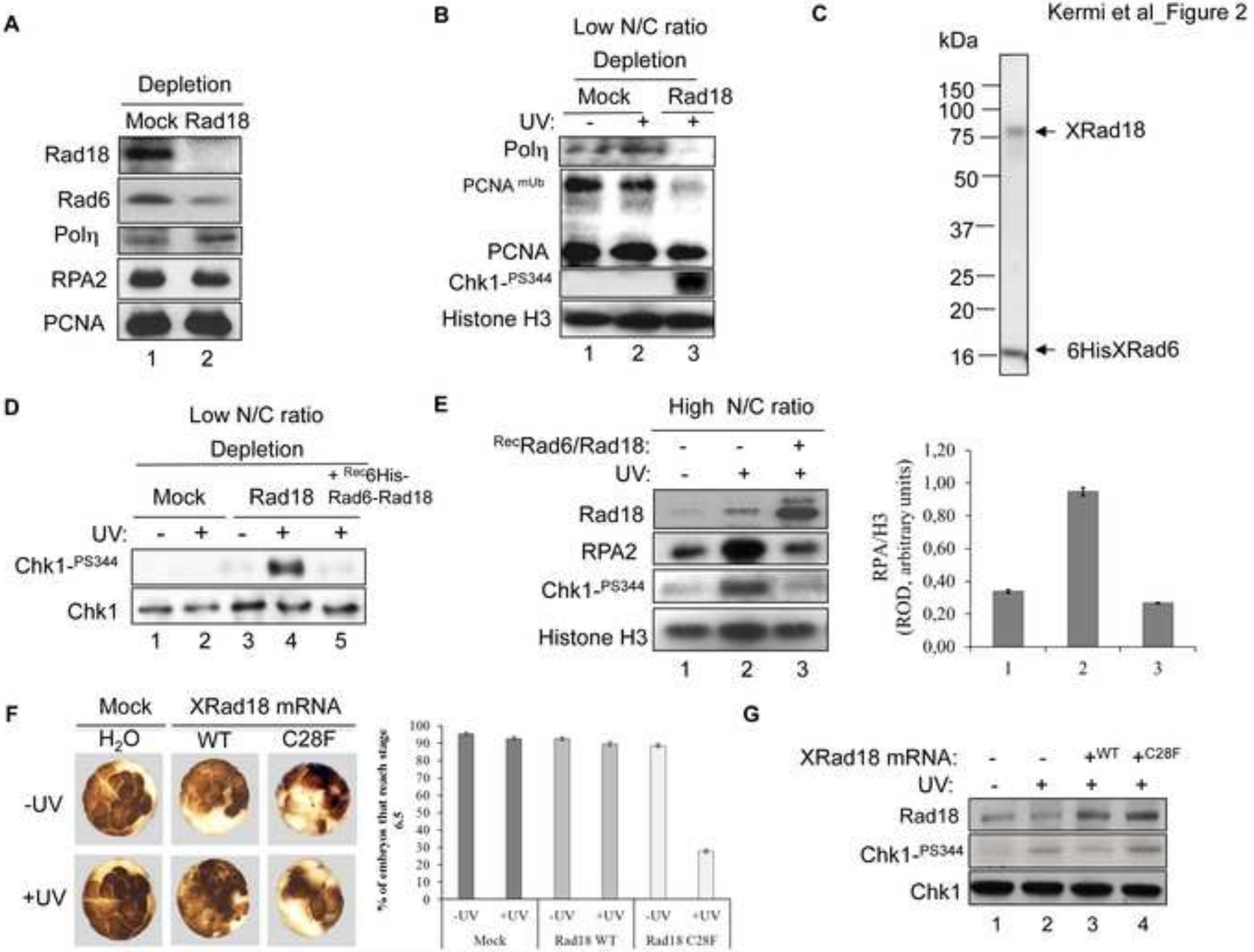

Figure3
Click here to download Figure: Figure3.tif

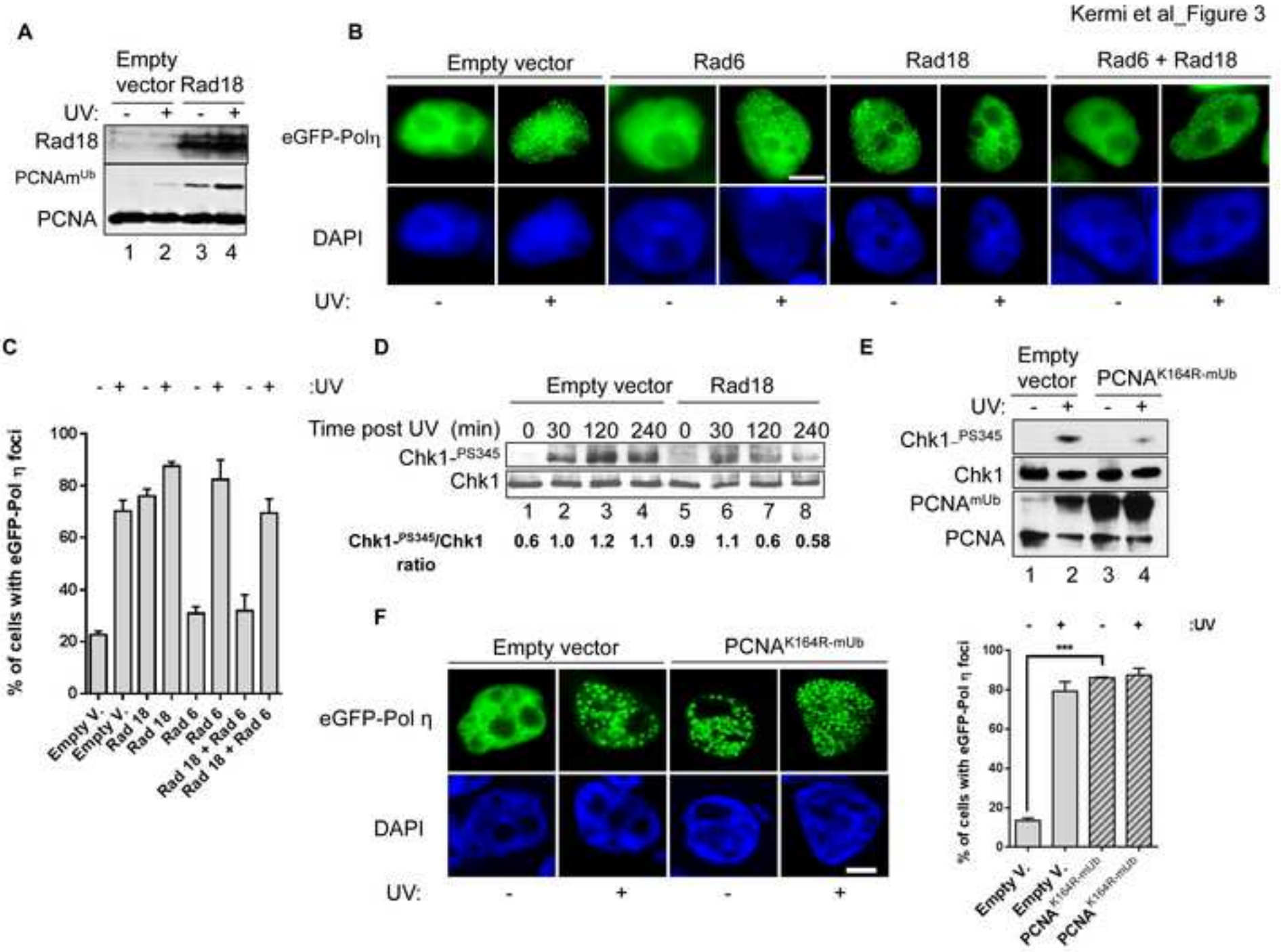

Figure4
Click here to download Figure: Figure4.tif

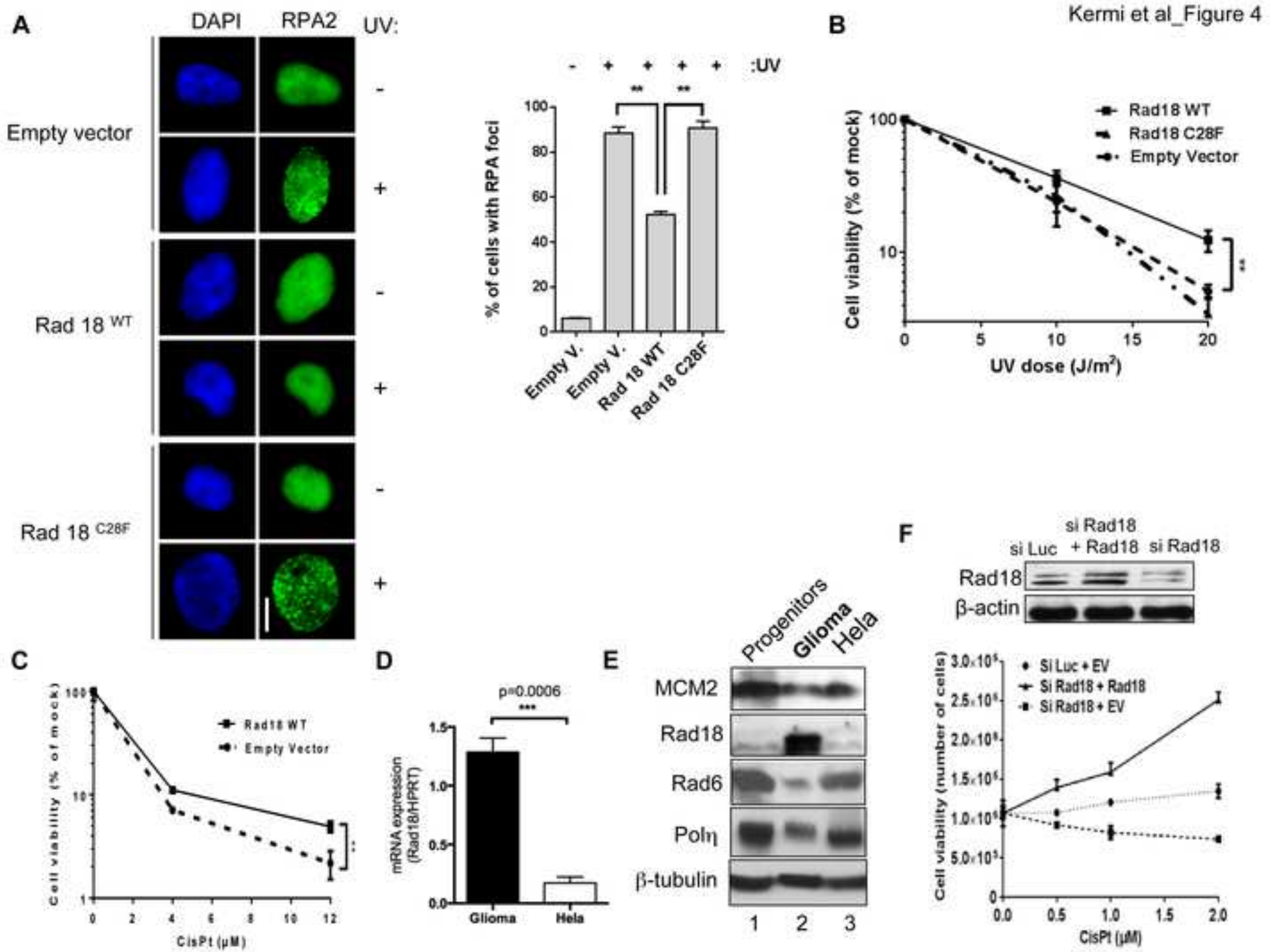

Rad18 is a maternal limiting factor silencing the UV-dependent DNA damage checkpoint in *Xenopus* embryos

Chames Kermi, Susana Prieto, Siem van der Laan, Nikolay Tsanov, Bénédicte Recolin, Emmanuelle Uro-Coste, Bernadette Delisle and Domenico Maiorano

INVENTORY OF SUPPLEMENTAL INFORMATION

This includes four Supplemental Figures S1-4 and legends, Supplemental Experimental Procedures, and sixteen supplemental references.

Figure S1 is related to Figure 1 because shows controls regarding the effect of the N/C ratio upon cell cycle progression in the presence of DNA damage and its relationships with replicative and translesion DNA polymerases in Xenopus egg extracts.

Figure S2 is related to Figure 2 and shows important controls about the specificity of Rad18 depletion on checkpoint activation at low N/C ratio as well as the contribution of $PCNA^{mUb}$ both *in vitro* and *in vivo* in Xenopus.

Figure S3 is related to Figure 3 and shows important controls about the specificity of the phenotypes observed upon Rad18 overexpression in mammalian cells.

Figure S4 is related to Figure 4 because shows the expression of rad18 in colorectal cancer cell lines sensitivie or resistant to oxaliplatin and the expression of divers DNA damage markers in glioblastoma.

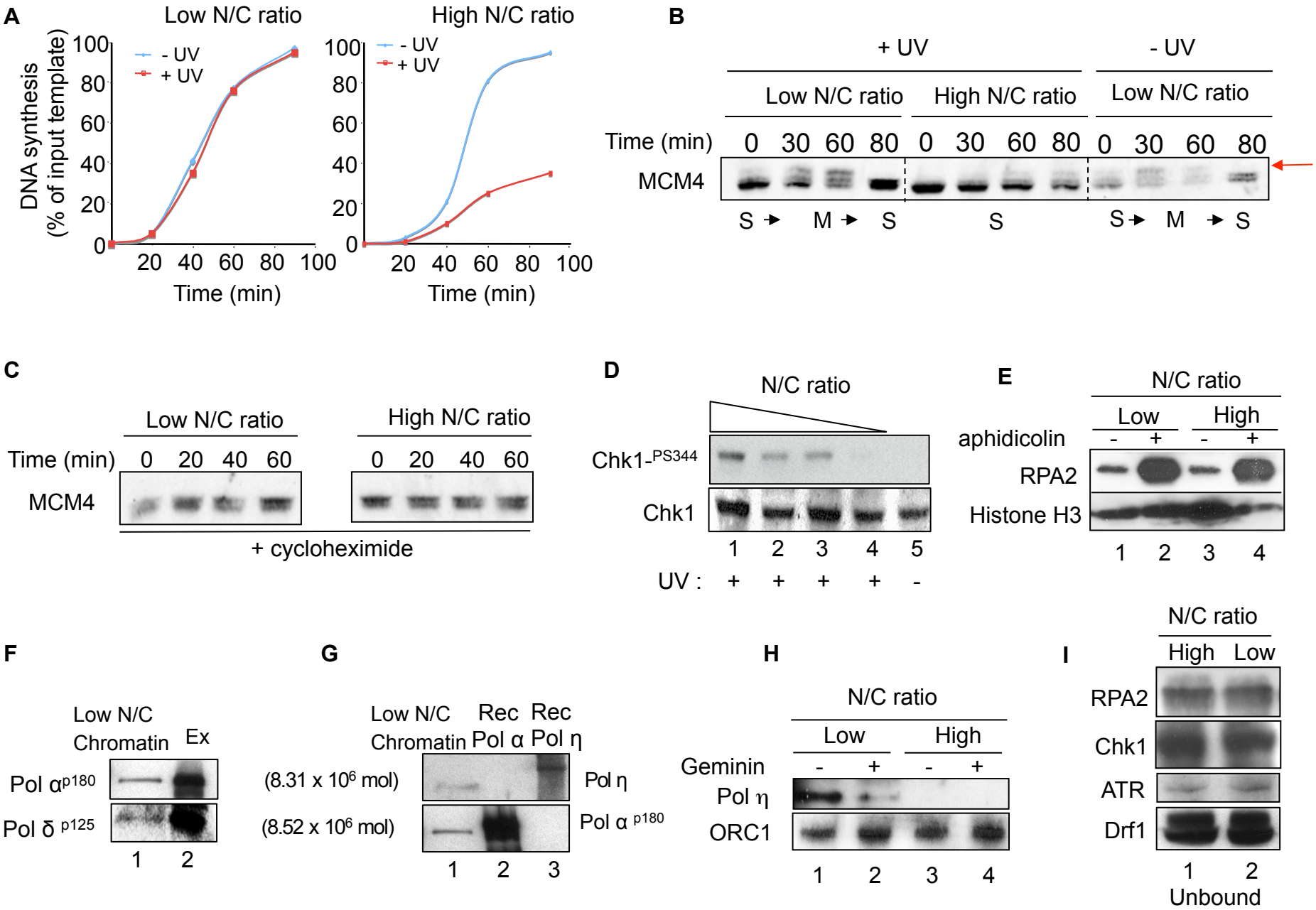
A
Low N/C ratio
High N/C ratio
DNA synthesis (% of input template)
- UV
+ UV
Time (min)
B
+ UV
- UV
Low N/C ratio
High N/C ratio
Low N/C ratio
Time (min)
0 30 60 80 0 30 60 80 0 30 60 80
MCM4
S → M → S
S
S → M → S
C
Low N/C ratio
High N/C ratio
Time (min)
0 20 40 60
0 20 40 60
MCM4
+ cycloheximide
D
N/C ratio
Chk1-PS344
Chk1
1 2 3 4 5
UV : + + + + -
E
N/C ratio
Low
High
aphidicolin
- + - +
RPA2
Histone H3
1 2 3 4
F
Low N/C Chromatin
Ex
Pol αp180
Pol δ p125
1 2
G
Low N/C Chromatin
Rec Pol α
Rec Pol η
(8.31 x 10^6 mol)
Pol η
(8.52 x 10^6 mol)
Pol α p180
1 2 3
H
N/C ratio
Low
High
Geminin
Pol η
ORC1
- + - +
1 2 3 4
I
N/C ratio
High Low
RPA2
Chk1
ATR
Drf1
1 2
Unbound

Kermi et al., Figure S2

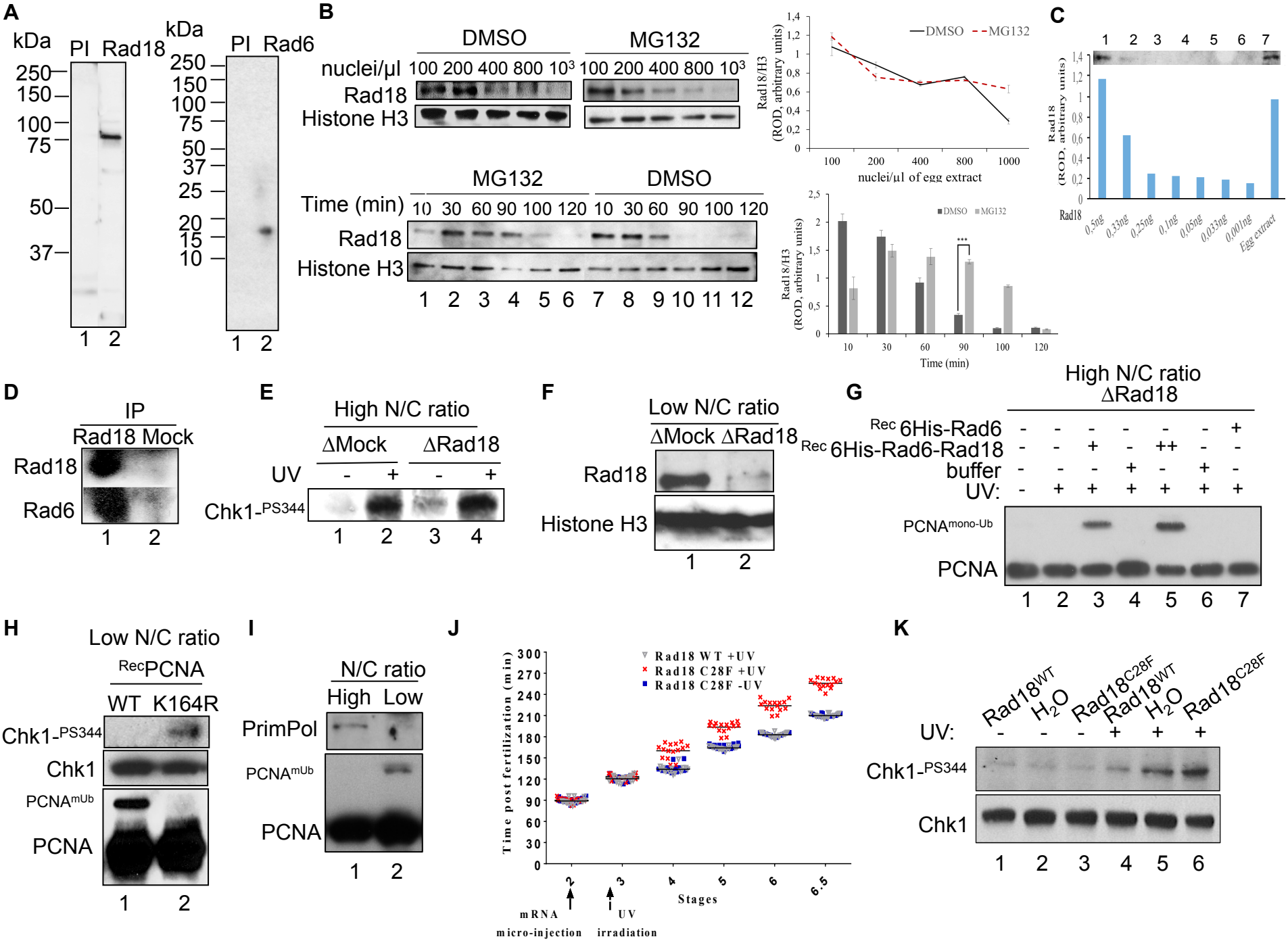

Kermi et al., Figure S3

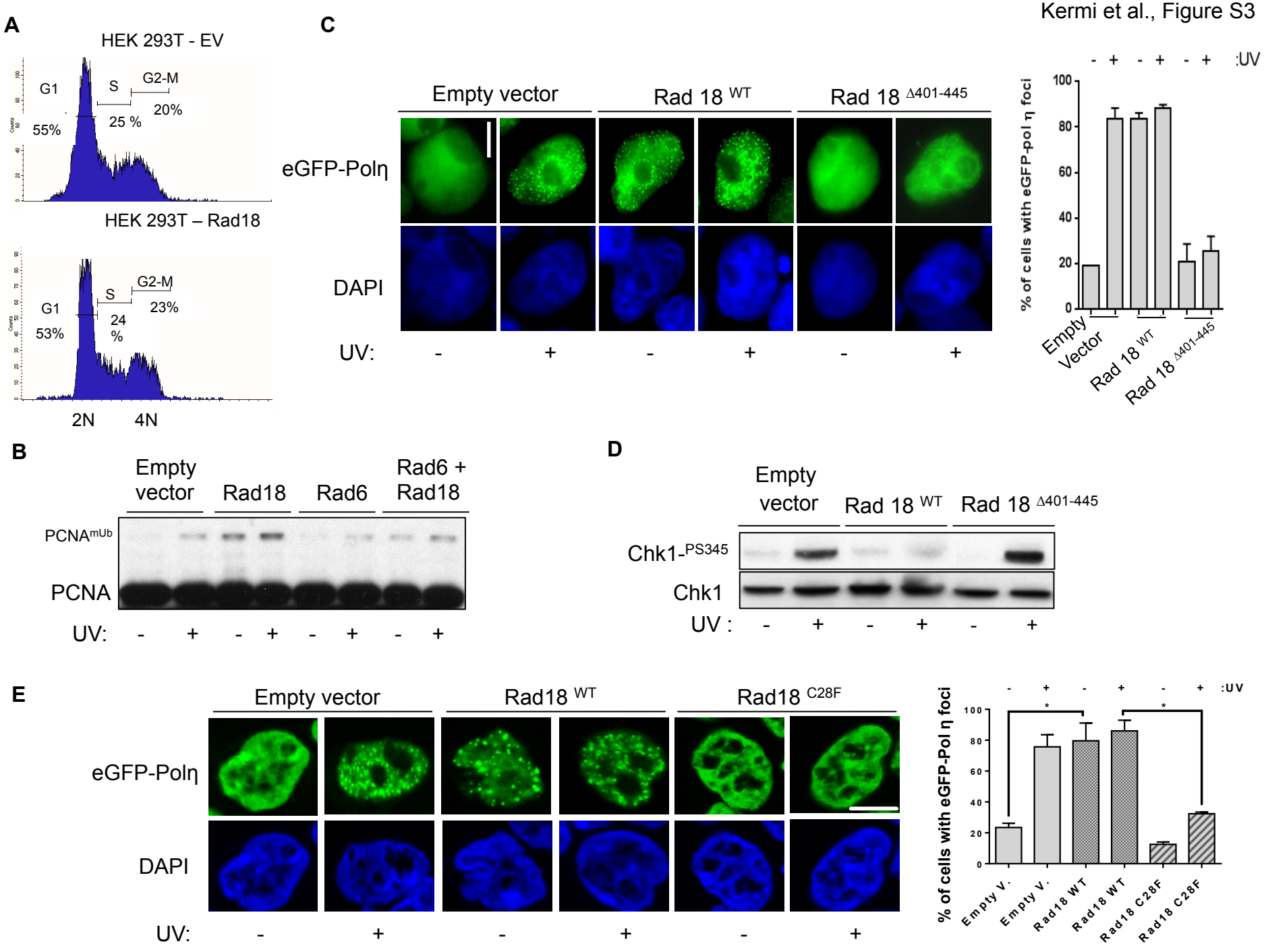

A

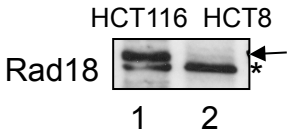
HCT116
HCT8
Rad18
*
1
2

B

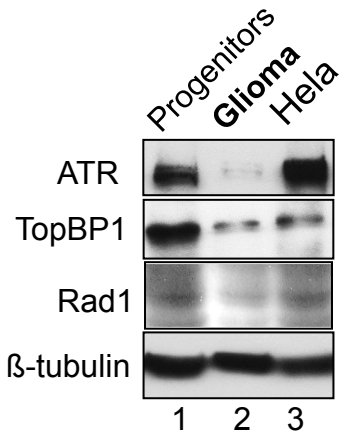
Progenitors
Glioma
Hela
ATR
TopBP1
Rad1
ß-tubulin
1
2
3

SUPPLEMENTAL INFORMATION

Supplemental Figures legend.

Figure S1, related to Figure 1

(A) DNA synthesis, monitored by incorporation of a nucleotide precursor, of egg extracts supplemented with sperm nuclei at low N/C ratio in the presence (+) or absence (-) of UV-irradiated chromatin (300 J/m^2).

(B) Cycling egg extracts were incubated at room temperature for the indicated times in the absence or presence (C) of cycloheximide and analysed by western blot to detect the phosphorylated forms of MCM4 (arrows), a CDK1 substrate (Hendrickson et al., 1996). UV irradiation did not induced mitotic delay, similar to the non-irradiated control (right panel). In contrast, extracts supplemented with sperm nuclei at high N/C ratio were strongly delayed in interphase (middle panel). No MCM4 phosphorylation was observed in the presence of cycloheximide at both low and high N/C ratio **(**C**)** as expected (Maiorano et al., 2004), due to inhibition of cyclin B synthesis, indicating failure to enter mitosis.

(D) Checkpoint suppression by decreasing the N/C ratio. Equal amounts of sperm nuclei (1000 nuclei/μl) UV-irradiated (lanes 1-4) or not (lane 5) were incubated at room temperature for sixty minutes with increasing volumes of egg extracts (dilution factors X3, X6, X9 respectively for lanes 2-4 compared to lane 1). Nuclei were then isolated and Chk1 phosphorylation analyzed by western blot with a specific antibody. Chk1 serves here as loading control.

(E) Aphidicolin induces replication fork uncoupling at low N/C ratio. Egg extracts were supplemented with sperm nuclei at low N/C ratio in the presence (+) or absence (-) of 100 μg/ml of aphidicolin. Chromatin fractions were isolated and analysed by western blot with the indicated antibodies.

(F) Association of replicative DNA polymerases α and δ catalytic subunits with chromatin at low N/C ratio. Western blot of chromatin fractions obtained at low N/C ratio and *Xenopus* egg extracts (LSS) with the indicated antibodies.

(G) Quantificatio of Polη binding to chromatin at low N/C ratio compared to recombinant Polη and Polα (Rec). Mol: number of molecules per replication unit.

(H) Chromatin binding of Polη at low N/C ratio is inhibited by Geminin. Chromatin binding was analysed as in (F) in the absence (-) or presence (+) of 100 nM of recombinant Geminin. ORC1 was used in this experiment as a chromatin loading control.

(I) Comparison of abundance of the indicated proteins (as determined by western blot) remaining in the egg cytoplasm after incubation with sperm chromatin at low or high N/C ratio. Egg extracts were supplemented with either 100 (low N/C ratio) or 1000 (high N/C ratio) nuclei/μl and incubated at room temperature for ninety minutes.

Figure S2, related to Figure 2

(A) Western blot of *Xenopus* egg extracts probed with either pre-immune (PI), Rad6 or Rad18 anti-serum. kDa indicates molecular weight standards.

(B) Effect of MG132 on Rad18 stability *in vitro*. (Upper panel) Titration of Rad18 onto chromatin by increasing the N/C ratio (nuclei/μl of egg extract) in the absence (DMSO) or presence of MG132. Western blot of chromatin sample taken at 70

minutes after incubation at room temperature and isolated as described in experimental procedures. Quantification is shown. Means and standard deviation of two independent experiments are shown. (Lower panel) Dynamics of Rad18 chromatin binding as described above. Quantification is shown. Means and standard deviation of two independent experiments are shown.

(C) Quantification of Rad18 stored in the *Xenopus* egg. Western blot of samples of recombinant XRad18 (lanes 1-7) and 1μl of *Xenopus* egg extract (~ 25 μg of total proteins, corresponding to about 2 embryos assuming that one egg yields about 0.5μl of extract) with the anti-Rad18 antibody. Ng indicates nanograms of recombinant Rad18. Western blot signals were quantified using the Image J software and expressed in the graph as relative optical density (ROD).

(D) Immunoprecipitation of Rad18 co-precipitates the Rad6 protein. Egg extracts were incubated with either mock or Rad18-specific antibodies for 1 hour at 4 °C and immunoprecipitates were analysed by western blot with the indicated antibodies.

(E) Rad18 depletion (ΔRad18), compared to control depletion (ΔMock), does not stimulate UV-dependent Chk1 phosphorylation at high N/C ratio. Analysis of $Chk1^{S344}$ phosphorylation at high N/C ratio of the experiment described in Figure 2D.

(F) Western blot of chromatin fractions isolated from *Xenopus* egg extracts incubated with sperm chromatin at low N/C ratio, after treatment with non-specific (ΔMock) or Rad18-specific (ΔRad18) antibodies.

(G) The Rad6-Rad18 recombinant complex rescues defective $PCNA^{mUb}$ of Rad18-depleted egg extracts. Egg extracts depleted of Rad18 (ΔRad18) were reconstituted (+) or not (-) with increasing amounts of a 6His-Rad6-Rad18 recombinant (Rec) complex (corresponding to + and ++ in the panel legend), or recombinant 6His-Rad6,

and sperm chromatin at high N/C ratio. $PCNA^{mUb}$ was determined by western blot on chromatin fractions isolated after incubation at room temperature for 90 minutes.

(H) $PCNA^{K164R}$ induces $Chk1^{S344}$ phosphorylation upon UV irradiation in *Xenopus* egg extracts at low N/C ratio. Analysis of Chk1 phosphorylation in egg extracts supplemented with either wild-type (WT) PCNA or PCNA mutated in the lysine 164 residue (K164R) and sperm nuclei at low N/C ratio.

(I) Primpol does not bind to chromatin at low N/C ratio in *Xenopus* egg extracts. Western blot of chromatin fractions isolated from *Xenopus* egg extracts incubated with sperm chromatin at high or low N/C ratio and analysed with either PCNA or Primpol antibodies.

(J) Cell cycle duration of live embryos injected with the indicated mRNA at the 2-cell stage, UV-irradiated (+UV) or not (-UV) at stage 3. Data are represented as scatter dot plot. Time points and medians are represented. Fifteen individual embryos were followed through early divisions until 300 min after the first cleavage. Each time point corresponds to the cleavage of an individual cell from embryos.

(K) Rad18 overexpression suppresses UV-dependent Chk1 phosphorylation in *Xenopus* embryos. Western blot of embryos protein extracts (from Figure 2F; see Experimental Procedures) obtained from embryos injected with the Rad18 mRNA or water (H_2O) and probed with the indicated antibodies.

Figure S3, related to Figure 3

(A) Cell cycle profile of cell overexpressing Rad18. FACS analysis of HEK293T cells expressing either the empty vector (EV) or Rad18. The percentage of cells in each cell cycle phase is shown. 2N and 4N indicate DNA content.

(B) Rad18 and not Rad6 stimulates $PCNA^{mUb}$ in mammalian cells. Western blot of total cell extracts of HEK293T cells expressing the indicated constructs described in Figure 3B and analysed with PCNA antibodies.

(C, left panel) HEK293T cells were co-transfected with HsRad18 wild-type or Rad18 missing the Cdc7 phosphorylation sites (Δ401-445 mutant) and a vector expressing the eGFP-Polη. Twenty-four hours later cell were UV-irradiated and processed for immunofluorescence microscopy as described in Experimental Procedures. Scale bar: 10μm. **(Right panel)** Quantification of eGFP-Polη foci from the experiment described in panel **C**. Means and standard deviation of three independent experiments are shown .

(D) Determination of $Chk1^{S345}$ phosphorylation in HEK293T cells expressing empty vector, $Rad18^{WT}$ or $Rad18^{\Delta 401-445}$, in the absence (-) or presence (+) of UV irradiation. Samples were analysed 240 minutes post-UV irradiation.

(E) HEK293T cells were co-transfected with empty vector, $HsRad18^{WT}$ or $Rad18^{C28F}$ mutant and a vector expressing the eGFP-Polη. Twenty-four hours later cell were UV-irradiated and processed for immunofluorescence microscopy as described in Experimental Procedures. Scale bar: 10μm. Quantification shows means and standard deviation of three independent experiments (*p<0.01).

Figure S4, related to Figure 4

(A) Expression of Rad18 in HCT116 and HCT8 colorectal cancer cell lines respectively resistant or sensitive to oxaliplatin treatement (Balin-Gauthier et al., 2008). Asterisk indicates a non-specific cross-reacting polypeptide.

(B) Expression of DNA damage response proteins in glioblastoma. Western blot of total extracts obtained from glioblastoma biopsies (Glioblstoma, grade 4) or differentiated counterparts (progenitors, CD133-) or Hela cells.

Supplemental Experimental Procedures

Cloning procedures and plasmids

A *X. tropicalis* Rad18 homologue (EST: AL881643) was identified in the databank by performing a BLAST search using human and mouse Rad18 proteins. Two oligonucleotides specific of XtRad18 were synthesized, XtR18F (5'-GGAATTCGTTCAAATGTATAATGCTCA-3') and XtR18R (5'-CTGAGCATTATACATTTGAACGAATTCC-3') containing a synthetic *Eco*RI restriction site (underlined), and used as primers in PCR reactions with 5' or 3' primers specific of a *X. laevis* ovary cDNA library made in lambda gt10 vector (Rebagliati et al., 1985). PCR products were blunt-end ligated to pRSET expression vector (Invitrogen) to generate XlRad18^{Nter} or XlRad18^{Cter}. Recombinant plasmids were sequenced on both strands. Full-length *X. laevis* Rad18 was kindly provided by K. Cimprich (Stanford University, USA). The sequence of the *X. laevis* Rad18 gene has been deposited to the EMBL genebank (accession number CCQ71719.2). The PCNA 6His-K164R mutant was generated as previously described (Chang et al., 2006). The *Xenopus* Rad6 gene was obtained from NIBB *Xenopus* cDNA Resource (NIB, Japan). Full length XRad6 cDNA was amplified by PCR using 5' (5'-CCCGGATCCATGTCCACCCC-3') and 3' (5'-CCCCTCGAGTTAGGAATCATTCCAACTTTGCTC-3')-specific primers containing a synthetic *Bam*HI or *Xho*I restriction site (underlined). The PCR product was cloned into the pFastBacHtb vector (Pharmingen) digested with the same restriction enzymes to obtain the recombinant plasmid pFastBac6HisXRad6. The cDNA was sequenced on both strands. *Xenopus* full-length Rad18 was cloned into the

pFastBac1 vector as the *Xho*I-*Bam*HI DNA fragment. The recombinant plasmid pFastBacXRad18 was sequenced on both strands. The HsRad18 Δ401-445 and Rad18 C28F mutants were previously described (Huang et al., 2009; Watanabe et al., 2004). The plasmid expressing PCNA(K164R)-Ubiquitin fusion was previously described (Kanao et al., 2015).

Expression of recombinant proteins

6His-XlRad18^{Cter} was expressed in the *E. coli* strain BL21 Star (DE3). Cells were grown at 37 °C over night and diluted 100-fold into fresh LB until OD^{600} reaches 0.6. Then cells were left to shake at room temperature for 30 minutes and the expression of the recombinant protein was induced by addition of 0.5 mM IPTG. Cultures were left to shake for 3 hours at room temperature and harvested by centrifugation. The PCNA 6His-K164R mutant was expressed and purified as previously described (Chang et al., 2006). A recombinant 6His-Rad6-Rad18 complex was expressed in baculovirus-infected cells and purified to homogeneity on a Nickel column as previously described (Watanabe et al., 2004), followed by gel filtration. Recombinant Geminin was expressed in bacteria and purified as previously described (Tada et al., 2001).

Antibodies

XlRad18 antibodies were raised against 6His-XlRad18^{Cter} (amino acids 243-496) expressed and purified in bacteria by nickel affinity chromatography (Qiagen). Crude serum was also affinity-purified by affinity chromatography using the same antigen used to immunize rabbits coupled to Sepharose by standard procedures. RPA2

antibodies were previously described (Cuvier et al., 2006). XPolη antibodies were raised against full recombinant protein expressed in bacteria as previously described (Yagi et al., 2005). Rad6 antibodies were generated by injection of rabbit with recombinant, baculovirus-expressd *Xenopus* Rad6. The following antibodies were also used: human phospho-Chk1 (Ser^{345}, Cell Signaling; 2341; recognizes S^{344} XChk1); Chk1 (G-4, sc-8408, Santa Cruz biotechnology); H3 (ab1791, AbCam); PCNA (PC10, Sigma); MCM4 (Coue et al., 1998); MCM2 (ab4461, AbCam), ß-tubulin (T3526, Sigma), USP1 (14346-1-AP, Proteintech); Drf1 (Yanow et al., 2003), Primpol (Wan et al., 2013). ATRIP was a kind gift of K. Cimprich (Stanford University, USA). ATR antibodies were raised as previously described (Hekmat-Nejad et al., 2000). ORC1 antibody was a gift of M. Méchali.

Immunodepletion procedures

Rad18 was removed from egg extracts by two rounds of depletion with affinity-purified Rad18 antibodies coupled to DynaBeads (Invitrogen). This procedure allows minimal dilution of the extracts during the depletion procedure avoiding spontaneous checkpoint activation likely due to dilution of the Rad6-Rad18 complex. Egg supernatants were thawed and supplemented with cycloheximide on ice and beads were added to the extract in a 50% ratio (V:V). For immunoprecipitations, extracts were diluted ten-fold in XB buffer supplemented with protease inhibitors and incubated with Rad18 antibody for 1 hour at 4°C. Immunocomplexes were collected with Protein A sepharose, washed in XB buffer and neutralized in Laemmli buffer.

RNA extraction, reverse transcription and quantitative real-time PCR

Total RNA was isolated with TRIzol reagent (Invitrogen). Reverse transcription was carried out using random hexanucleotides (Sigma) and Superscript II First-Strand cDNA synthesis kit (Invitrogen). Quantitative PCR reactions were performed using Lightcycler SYBR Green I Master mix (Roche) on Lightcycler apparatus (Roche). All primers used were intron spanning and to ensure specificity melt-curve analysis were carried out at the end of all PCR reactions (primer sequences available upon request). The relative amount of target cDNA was obtained by normalisation using geometric averaging of an internal control gene (HPRT, Hypoxanthine-Guanine Phosphoribosyl Transferase).

Patients and tumour samples.

Tumour sample were obtained from patients diagnosed for type IV grade glioma (i.e. glioblastoma) and undergoing surgery at the neurosurgery department of the Rangueil Hospital (Toulouse, France). All subjects provided their informed written consent before their surgery and the protocol followed the declaration of Helsinki guidelines and was approved by local ethics committee.

Supplemental References

Balin-Gauthier, D., Delord, J.P., Pillaire, M.J., Rochaix, P., Hoffman, J.S., Bugat, R., Cazaux, C., Canal, P., and Allal, B.C. (2008). Cetuximab potentiates oxaliplatin cytotoxic effect through a defect in NER and DNA replication initiation. British journal of cancer *98*, 120-128.

Balin-Gauthier, D., Delord, J.P., Pillaire, M.J., Rochaix, P., Hoffman, J.S., Bugat, R., Cazaux, C., Canal, P., and Allal, B.C. (2008). Cetuximab potentiates oxaliplatin cytotoxic effect through a defect in NER and DNA replication initiation. British journal of cancer *98*, 120-128.

Chang, D.J., Lupardus, P.J., and Cimprich, K.A. (2006). Monoubiquitination of proliferating cell nuclear antigen induced by stalled replication requires uncoupling of DNA polymerase and mini-chromosome maintenance helicase activities. J Biol Chem *281*, 32081-32088.
Coue, M., Amariglio, F., Maiorano, D., Bocquet, S., and Mechali, M. (1998). Evidence for different MCM subcomplexes with differential binding to chromatin in Xenopus. Exp Cell Res *245*, 282-289.
Cuvier, O., Lutzmann, M., and Mechali, M. (2006). ORC is necessary at the interphase-to-mitosis transition to recruit cdc2 kinase and disassemble RPA foci. Curr Biol *16*, 516-523.
Hekmat-Nejad, M., You, Z., Yee, M.C., Newport, J.W., and Cimprich, K.A. (2000). Xenopus ATR is a replication-dependent chromatin-binding protein required for the DNA replication checkpoint. Curr Biol *10*, 1565-1573.
Hendrickson, M., Madine, M., Dalton, S., and Gautier, J. (1996). Phosphorylation of MCM4 by cdc2 protein kinase inhibits the activity of the minichromosome maintenance complex. Proc Natl Acad Sci USA *93*, 12223-11228.
Huang, J., Huen, M.S., Kim, H., Leung, C.C., Glover, J.N., Yu, X., and Chen, J. (2009). RAD18 transmits DNA damage signalling to elicit homologous recombination repair. Nat Cell Biol *11*, 592-603.
Kanao, R., Masuda, Y., Deguchi, S., Yumoto-Sugimoto, M., Hanaoka, F., and Masutani, C. (2015). Relevance of simultaneous mono-ubiquitinations of multiple units of PCNA homo-trimers in DNA damage tolerance. PLoS One *10*, e0118775.
Maiorano, D., Rul, W., and Mechali, M. (2004). Cell cycle regulation of the licensing activity of Cdt1 in Xenopus laevis. Exp Cell Res *295*, 138-149.
Rebagliati, M.R., Weeks, D.L., Harvey, R.P., and Melton, D.A. (1985). Identification and cloning of localized maternal RNAs from Xenopus eggs. Cell *42*, 769-777.
Tada, S., Li, A., Maiorano, D., Mechali, M., and Blow, J.J. (2001). Repression of origin assembly in metaphase depends on inhibition of RLF- B/Cdt1 by geminin. Nat Cell Biol *3*, 107-113.
Wan, L., Lou, J., Xia, Y., Su, B., Liu, T., Cui, J., Sun, Y., Lou, H., and Huang, J. (2013). hPrimpol1/CCDC111 is a human DNA primase-polymerase required for the maintenance of genome integrity. EMBO reports *14*, 1104-1112.
Watanabe, K., Tateishi, S., Kawasuji, M., Tsurimoto, T., Inoue, H., and Yamaizumi, M. (2004). Rad18 guides poleta to replication stalling sites through physical interaction and PCNA monoubiquitination. EMBO J *23*, 3886-3896.
Yagi, Y., Ogawara, D., Iwai, S., Hanaoka, F., Akiyama, M., and Maki, H. (2005). DNA polymerases eta and kappa are responsible for error-free translesion DNA synthesis activity over a cis-syn thymine dimer in Xenopus laevis oocyte extracts. DNA Repair (Amst) *4*, 1252-1269.
Yanow, S.K., Gold, D.A., Yoo, H.Y., and Dunphy, W.G. (2003). Xenopus Drf1, a regulator of Cdc7, displays checkpoint-dependent accumulation on chromatin during an S-phase arrest. The Journal of biological chemistry *278*, 41083-41092.